



# Anisotropic recombination of an immobilized photoinduced radical pair in a 50- $\mu$ T magnetic field: a model avian photomagnetoceptor

F. Cintolesi<sup>a</sup>, T. Ritz<sup>b,1</sup>, C.W.M. Kay<sup>c</sup>, C.R. Timmel<sup>a</sup>, P.J. Hore<sup>a,\*</sup>

<sup>a</sup> *Physical and Theoretical Chemistry Laboratory, Oxford University, South Parks Road, Oxford OX1 3QZ, UK*

<sup>b</sup> *Department of Biology, Virginia Tech., Blacksburg, VA 24061, USA*

<sup>c</sup> *Institut für Experimentalphysik, Freie Universität Berlin, Arnimallee 14, 14195 Berlin, Germany*

Received 25 March 2003

## Abstract

It has been suggested that chemical reactions proceeding through radical pair intermediates could form the basis of bird's ability to sense the geomagnetic field as a source of compass information [Biophys. J. 78 (2000) 707]. We present calculations of anisotropic reaction product yields for a flavin–tryptophan radical pair subject to a magnetic field of  $\sim 50 \mu\text{T}$ . The anisotropic response of the reaction is found to be dominated by two nitrogen nuclei in the flavin radical which have near-axial hyperfine interactions with almost collinear principal axes. It is shown that the anisotropy of the product yields is not strongly dependent on the lifetime of the radical pair in the range 1–5  $\mu\text{s}$ , and that it can be tuned by small variations in the hyperfine tensors of the nuclear spins in the two radicals.

© 2003 Elsevier B.V. All rights reserved.

## 1. Introduction

The Radical Pair Mechanism (RPM) is the only well-established mechanism by which magnetic fields can alter the rates and product yields of chemical reactions (for reviews see [1–5]). RPM magnetic field effects have been exploited extensively over the last 30 years to probe the structural,

dynamic and chemical properties of free radical reactions in solution [2] and in natural [1,3] and artificial [6] photosynthetic systems. The RPM has been discussed as a possible source of adverse health effects of electromagnetic fields [7] and has been proposed as the basis of birds' ability to sense the geomagnetic field as a means of orientation [8–10]. This last idea has recently been revived by Ritz et al. [11] who argue that a RPM magnetoreceptor is a viable alternative to hypotheses based on ferromagnetic material [12,13] as it could explain many of the properties of the avian compass: that it detects the inclination rather than the polarity of the geomagnetic field, that it is dependent on the wavelength of the ambient light, and that it is

\* Corresponding author. Tel.: +44-1865-275415; fax: +44-1865-275410.

E-mail address: [peter.hore@chem.ox.ac.uk](mailto:peter.hore@chem.ox.ac.uk) (P.J. Hore).

<sup>1</sup> Present address: Department of Physics and Astronomy, University of California, Irvine, CA 92697-4575, USA.

sensitive to a narrow range of magnetic field strengths [14,15].

At the heart of the RPM is a pair of transient radicals created in an electronic singlet ( $S$ ; anti-parallel electron spins) or triplet ( $T$ ; parallel electron spins) state. For a radical pair to respond to an applied magnetic field, the  $S$  and  $T$  states must have different chemical fates – the reactivity of the pair should be spin-dependent – and there must be magnetic electron–nuclear hyperfine interactions in one or both radicals, which drive the coherent oscillatory interconversion of  $S$  and  $T$  states on a nanosecond timescale. The fraction of radical pairs that recombine from the  $S$  state, for example, depends on a competition between the separate reactions of the two states, regulated by the  $S \leftrightarrow T$  interconversion process. The sensitivity to an applied magnetic field arises because the efficiency and frequency of the  $S \leftrightarrow T$  interconversion is not only driven by intrinsic magnetic interactions but is also influenced by the Zeeman interactions of the electrons. If the correlation between the two electron spins persists for as long as  $\sim 1 \mu\text{s}$ , the radical pair product yields can be modified by applied magnetic fields as weak as  $\sim 50 \mu\text{T}$ , the approximate strength of the Earth's field [16]. Under appropriate conditions the response of a radical pair reaction to an external magnetic field is biphasic, with a so-called Low Field Effect at field strengths less than or similar to the magnitude of the hyperfine interactions [7,16–19]. The origin of the LFE has been shown to lie in the removal of degeneracies amongst the spin energy levels of the radical pair by the electron Zeeman interactions [16].

The Ritz–Schulten proposal is that a radical pair is created photochemically in the bird's retina by a photoinduced electron transfer reaction between cofactors embedded in an immobilised protein [11]. The source of the orientation information, it is suggested, lies in the anisotropy of the hyperfine interactions which cause the interconversion of  $S$  and  $T$  states and hence the product yields to depend on the orientation of the radical pair and therefore of the bird's head with respect to the magnetic field direction. This primary reception process might be connected to the nervous system in one of two ways [11]: either the radical

pair process could affect the sensitivity of light receptors in the eye (and thus benefit from the amplification mechanisms involved in vision) or a decay product of the radical pair could be a neurotransmitter (in which case the amplification would depend on the number of neuroreceptors). Ritz et al. [11] propose that an electron transfer between the flavin cofactor of cryptochromes, a recently discovered class of vertebrate photoreceptors, and an as yet unknown second cofactor could form the magnetosensitive radical pair.

To provide a proof of principle that a radical pair reaction can act as a geomagnetic compass, Ritz et al. [11] show, by means of computer simulations, that a model radical pair in a  $50\text{-}\mu\text{T}$  field can have significantly anisotropic recombination product yields. They treat a pair of radicals each of which contains a single spin-1/2 magnetic nucleus: one of the hyperfine interactions is anisotropic with axial symmetry and the other is isotropic. In agreement with previous studies of (isotropic) effects of weak magnetic fields [16], they find that the recombination yield is sensitive to the field strength  $B_0$  and the value of the recombination rate constant  $k$  relative to the size of the hyperfine interactions; the longer lived the pair the more sensitive it is to changes in  $B_0$ . Moreover, significant orientation dependence of the product yields was found for values of  $B_0$  between 0 and  $250 \mu\text{T}$  using  $k = 10^6 \text{ s}^{-1}$ . Similar anisotropic effects were subsequently reported by Timmel et al. for one-nucleus radical pairs with an axial or biaxial hyperfine tensor and a variety of rate constants. Recombination yields for such prototype radical pairs were predicted to vary by up to 40% as a function of orientation [20].

Encouraging though these calculations are, they could be criticised for focussing on radicals containing an unrealistically small number of nuclear spins. Any radicals generated by photoinduced electron transport from cofactors in a protein are likely to have many significant hyperfine interactions, even if those radicals have evolved to be exquisitely sensitive to the geomagnetic field. To take an example, the ubisemiquinone radical anion that forms part of the secondary photoinduced radical pair in the photosynthetic bacterium *Rhodospira rubra* has five protons with isotro-

pic hyperfine couplings larger than 50  $\mu\text{T}$  [21]. The counter-radical in this pair, a bacteriochlorophyll dimer cation, has even more [22]. In the absence of computer simulations, it is difficult to extrapolate from the model systems hitherto studied to more realistic multi-nuclear radical pairs. It would be difficult to argue plausibly, for example, that a system with many hyperfine interactions, each with a different axially and biaxially and different principal axes, could be expected to show recombination yield anisotropies as large as the 40% noted above. One might expect that the effects of the various hyperfine anisotropies would cancel one another to some degree leading to a much more nearly isotropic response to an external magnetic field.

In this paper we calculate the field-, orientation- and lifetime-dependence of the recombination yields of one particular multi-nuclear radical pair. Although cryptochromes have been proposed as radical pair magnetoreceptors [11], there is as yet little or no experimental evidence for the hypothesis. While it is known that cryptochromes contain the highly redox-active cofactor flavin adenine dinucleotide, FAD [23], no radical pairs involving cryptochromes have been found that could provide suggestions for the identity of the second cofactor in the radical pair. Faced with this lack of information, it would be tempting to embark on a systematic investigation of radical pairs with progressively increasing numbers of nuclear spins. We have gone a small distance along this road, by studying a variety of two-proton radical pairs with different combinations of isotropic, axial and biaxial hyperfine tensors [24]. Brocklehurst has performed similar calculations [25]. The results, even for such a small number of nuclei, are dauntingly complex and have proved difficult to generalise. The prospects for extending this approach to radical pairs containing three or more nuclei do not seem very hopeful. An alternative strategy would be to select an arbitrary pair of radicals to get a sense of how the properties of a large spin system might differ from those of the prototype radical pairs studied hitherto. Rather than generate hyperfine tensor parameters at random, we have chosen a system based on a photoinduced radical pair produced in *Escherichia coli* DNA

photolyase [26–33], a member of a class of enzymes which are highly homologous to cryptochromes and contain the same FAD cofactor [34].

Photolyases are photoactive enzymes that repair damaged DNA by splitting cyclobutane pyrimidine dimers. At least two types of photoreactions have been observed: (1) photorepair of DNA by the catalytically active enzyme containing the flavin cofactor in its fully reduced state,  $\text{FADH}^-$  [27,32,33,35] and (2) photoactivation of the catalytically inert enzyme when the flavin is either semi-reduced to  $\text{FADH}^\cdot$  or fully oxidised to FAD [36–42]. The latter proceeds via an electron transfer chain involving the photoexcited triplet state of the flavin and a series of electron donors all three of which are tryptophan residues. The final radical pair so formed is believed to involve a Trp-306 radical, which is re-reduced on a millisecond timescale by back electron transfer from the flavin radical situated 1.4 nm away. Time resolved electron paramagnetic resonance experiments [38,42] have detected a photoinduced EPR signal with a  $\sim 20 \mu\text{s}$  lifetime displaying the antiphase lineshapes that are diagnostic of a spin-correlated radical pair [43].

Inspired by these observations, we have performed extensive calculations of anisotropic magnetic field effects for a radical pair comprising non-interacting flavin and tryptophan radicals, taking hyperfine coupling data for the two radicals from EPR and ENDOR experiments and density functional calculations. Our aim has been to explore the sensitivity of a radical pair of realistic complexity to the strength and direction of an Earth-strength magnetic field. It should be emphasized at the outset that it has not been our intention accurately to model the photoactivation reaction in DNA photolyase, nor to suggest that cryptochromes can harbour flavin–tryptophan radical pairs. Indeed, it has recently been shown that in the related (6-4) photolyases, photoactivation proceeds via a flavin–tyrosine radical pair [44], whereas at the present time there is no information on such processes in cryptochromes. Nevertheless, given that the first cryptochrome structure to be elucidated [45] shows strong similarities to the structures of photolyases [36,46,47], we consider that the results described here make a

strong case for the idea that a light-induced “flavin–amino acid” radical pair could be involved in magnetic field sensing.

## 2. Methods

Calculations have been performed using the following model of a protein–bound radical pair, formed by photoinduced electron transfer in a static environment devoid of molecular motion. (a) The radical pair comprises two radicals A and B, each of which has a single unpaired electron and several magnetic nuclei which either have spin quantum number  $I = 1/2$  ( $^1\text{H}$ ) or  $I = 1$  ( $^{14}\text{N}$ ). (b) The radical pair is in a pure  $S$  state at the moment of its creation at time  $t = 0$  and the radicals are far enough apart ( $> \sim 3$  nm) that spin–spin interactions (exchange and dipolar) between the two electrons can be neglected. (c) The radical pair is able to recombine with first order kinetics from both its  $S$  and  $T$  states with a rate constant  $k$ . (d) Coherent  $S \leftrightarrow T$  interconversion is driven by both the anisotropic hyperfine couplings within the two radicals and the Zeeman interactions of the two electrons with the applied magnetic field  $B_0$ . This evolution is described by a spin Hamiltonian  $\hat{H} = \hat{H}_A + \hat{H}_B$ , where the individual radical Hamiltonians,  $\hat{H}_A$  and  $\hat{H}_B$ , commute. Any spin evolution arising from the nuclear Zeeman interactions, the difference between the two isotropic  $g$ -values, or  $g$ -tensor anisotropy is considered negligible at the weak field strengths ( $0 < B_0 < 200$   $\mu\text{T}$ ) considered. Nuclear quadrupolar interactions, which are likely to be similar in size to the hyperfine interactions for the  $^{14}\text{N}$  nuclei, are also ignored. The role of quadrupolar interactions in magnetic field effects is unclear and will be the subject of further study.

The aim is to calculate the time-dependent probability  $p_S(t)$  that the radical pair is in a singlet state and hence the fraction of pairs that have recombined via the  $S$  state in the limit  $t \rightarrow \infty$ . The reaction considered is shown schematically in Fig. 1. The singlet probability is a sum of damped oscillations at frequencies characteristic of the magnetic interactions in the radical pair [16]:

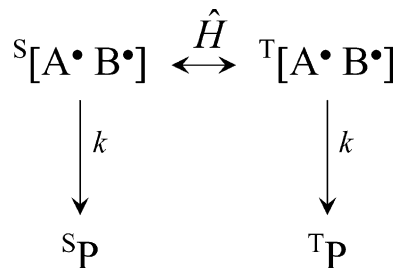


Fig. 1. Reaction scheme for a photoinduced radical pair,  $A\cdot B\cdot$ , formed in a singlet ( $S$ ) state and able to react via the singlet or triplet ( $T$ ) states to give chemically distinct products,  $^S\text{P}$  and  $^T\text{P}$ , respectively, and to interconvert under the influence of the spin Hamiltonian,  $\hat{H}$ .

$$p_S(t) = \frac{1}{M} \sum_{j=1}^{4M} \sum_{l=1}^{4M} \left| \langle j | \hat{P}^S | l \rangle \right|^2 \cos \omega_{jl} t e^{-kt}, \quad (1)$$

where  $\hat{P}^S$  is the singlet projection operator and  $M$  is the number of nuclear spin configurations ( $M = 2^n 3^m$  for a radical pair with  $n$   $^1\text{H}$  and  $m$   $^{14}\text{N}$  nuclei). The indices  $j$  and  $l$  label the  $4M$  eigenstates of  $\hat{H}$ . The  $S \leftrightarrow T$  interconversion frequencies are differences between pairs of eigenvalues of  $\hat{H}$ :  $\omega_{jl} = \omega_j - \omega_l$ .

The projection operator  $\hat{P}^S$  can be written in terms of the Cartesian components of the spin angular momentum operators for the two electrons,  $\hat{S}_{Ap}$  and  $\hat{S}_{Bp}$  ( $p = x, y, z$ ) and  $\hat{E}$ , the identity operator:

$$\hat{P}^S = \frac{1}{4} \hat{E} - \sum_{p=x,y,z} \hat{S}_{Ap} \hat{S}_{Bp}. \quad (2)$$

Hence [19]:

$$p_S(t) e^{kt} = \frac{1}{4} + \frac{1}{M} \sum_m \sum_n \sum_r \sum_s g_{nm}^A g_{rs}^B \times \cos(\omega_{mn}^A - \omega_{rs}^B) t, \quad (3)$$

where

$$g_{jk}^C = \sum_{p=x,y,z} \sum_{q=x,y,z} (\hat{S}_{Cq})_{jk} (\hat{S}_{Cp})_{kj}, \quad C = A \text{ or } B \quad (4)$$

and the frequencies  $\omega_{mn}^A$  and  $\omega_{rs}^B$  are differences between pairs of eigenvalues of  $\hat{H}_A$  and  $\hat{H}_B$ , respectively:  $\omega_{jl}^C = \omega_j^C - \omega_l^C$ ,  $C = A$  or  $B$ .

The fraction of radical pairs that recombine via the singlet channel is then calculated as the integral of  $p_S(t)$ ,

$$\begin{aligned} \Phi_S &= k \int_0^\infty P_S(t) dt \\ &= \frac{1}{4} + \frac{1}{M} \sum_m \sum_n \sum_r \sum_s g_{nm}^A g_{rs}^B \\ &\quad \times \frac{k^2}{k^2 + (\omega_{mn}^A - \omega_{rs}^B)^2}. \end{aligned} \quad (5)$$

With the available computational resources this approach allowed us to include up to eight nuclei in the radical pair, with up to five in one radical.

For a radical pair that starts in a triplet (rather than a singlet) state, the probability of recombining from the singlet state is  $\frac{1}{3}(1 - \Phi_S)$  with  $\Phi_S$  given by Eq. (5). Note that Ritz et al. [11] calculated the recombination probability from the triplet state,  $\Phi_T$ , which is simply  $1 - \Phi_S$ .

The spin Hamiltonians for the two radicals have the form:

$$\begin{aligned} \hat{H}_C &= \omega_0(\sin \theta \cos \phi \hat{S}_{Cx} + \sin \theta \sin \phi \hat{S}_{Cy} + \cos \theta \hat{S}_{Cz}) \\ &\quad + \sum_i \hat{S}_C \cdot A_i \cdot \hat{I}_i \quad C = A \text{ or } B, \end{aligned} \quad (6)$$

where  $\omega_0$  is the Larmor frequency of an electron with the free electron  $g$ -value,  $g_e$ , subject to the

applied field,  $\omega_0 = g_e \mu_B B_0 / \hbar$ .  $A_i$  and  $\hat{I}_i$  are, respectively, the hyperfine tensor and spin angular momentum operator for nucleus  $i$ .  $\hat{S}_A$  and  $\hat{S}_B$  are the spin angular momentum operators for the two electrons. The direction of the applied magnetic field with respect to a radical pair-fixed axis system is defined in terms of the polar angles  $\theta$  and  $\phi$ .  $\Phi_S$  was calculated for 64 equally spaced values of  $\theta$  and of  $\phi$  in the ranges  $\{0, \pi\}$  and  $\{0, 2\pi\}$ , respectively.

Fig. 2 shows the structures of the two radicals and their relative orientations. The isotropic hyperfine coupling constants and the principal values and axes of the anisotropic hyperfine tensors used in the calculations are given in Table 1. The data for the neutral flavin radical (FH $\cdot$ ) were obtained by Weber et al. [48,49] using EPR, ENDOR and density functional theory with the B3LYP functional as implemented in Gaussian 98 [50]. The calculations used heavy atom coordinates for FADH $\cdot$  from the crystal structure of *E. coli* DNA photolyase (Protein Data Bank entry 1DNP) [36]. Protons were then added and the geometry of the whole molecule optimized in vacuo. The FH $\cdot$  hyperfine tensor axes are quoted in the co-ordinate

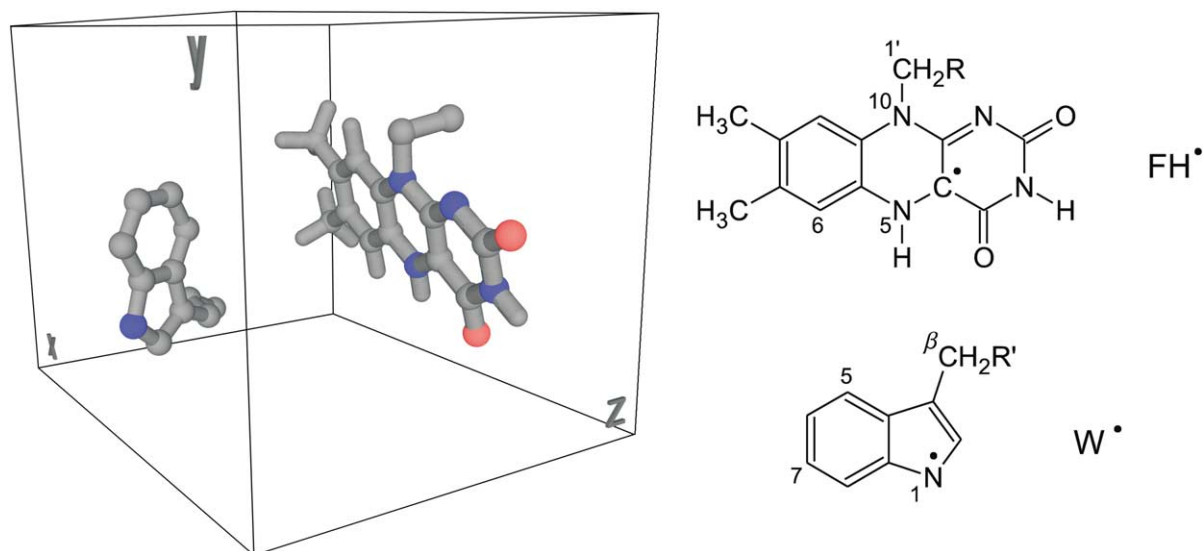


Fig. 2. Structures and numbering scheme for the neutral flavin radical FH $\cdot$  and the neutral tryptophan radical W $\cdot$ . The ball and stick structures shows the relative orientation of the two radicals and the coordinate system used in the calculations of anisotropic magnetic field effects.

Table 1

Isotropic hyperfine coupling constants ( $a_{\text{iso}}$ ), principal values of the anisotropic part of the hyperfine tensors ( $T_{ii}$ ,  $i = 1$  to 3) and principal hyperfine axes for nuclei in the neutral flavin (FH $\cdot$ ) and tryptophan (W $\cdot$ ) radicals

Radical	Nucleus	$a_{\text{iso}}$	$T_{ii}$	Principal hyperfine axes		
FH $\cdot$	N5	0.393	-0.498	0.4380	0.8655	-0.2432
			-0.492	0.8981	-0.4097	0.1595
			0.989	-0.0384	0.2883	0.9568
	N10	0.212	-0.242	0.9703	-0.2207	0.0992
			-0.234	0.2383	0.9426	-0.2340
			0.476	-0.0419	0.2506	0.9672
	H1'r	0.390	-0.062	-0.1902	0.3965	0.8981
			-0.033	0.9156	0.4017	0.0165
			0.095	-0.3542	0.8255	-0.4395
	H6	-0.158	-0.060	-0.0362	0.2937	0.9552
			-0.044	0.7948	0.5879	-0.1507
			0.104	-0.6059	0.7537	-0.2546
	H5	-0.769	-0.616	0.9819	0.1883	-0.0203
			-0.168	-0.0348	0.2850	0.9579
			0.784	-0.1861	0.9398	-0.2864
W $\cdot$	N1	0.40	-0.33	1.000	0.000	0.000
			-0.33	0.000	1.000	0.000
			0.66	0.000	0.000	1.000
	H $\beta$ 1	1.36	0.00	1.000	0.000	0.000
			0.00	0.000	1.000	0.000
			0.00	0.000	0.000	1.000
	H $\beta$ 2	2.83	0.00	1.000	0.000	0.000
			0.00	0.000	1.000	0.000
			0.00	0.000	0.000	1.000
	H5	-0.40	-0.23	-0.984	0.180	0.000
			0.35	0.180	0.984	0.000
			-0.12	0.000	0.000	1.000
	H7	-0.36	0.30	0.888	0.460	0.000
			-0.20	-0.460	0.888	0.000
			-0.10	0.000	0.000	1.000

All hyperfine coupling parameters are in mT.

system indicated in Fig. 2 (which is that of the geometry-optimised structure). The data for the oxidized neutral tryptophan radical (W $\cdot$ ) were taken from EPR and ENDOR measurements by Lenzian et al. [51] for Trp-111 in the *E. coli* ribonuclease reductase mutant R2 Y122F. The W $\cdot$  hyperfine tensor axes are quoted in molecule-based coordinates in which the  $z$ -axis is normal to the indole plane and the  $y$ -axis is parallel to the C5–C8 direction. The relative orientations of FH $\cdot$  and W $\cdot$  are those of FADH and Trp-306 in *E. coli* DNA photolyase [36] (see Fig. 2). In the following, nuclei are identified using a notation in which F(N5) is the nitrogen at position 5 in the flavin radical and W(H7) is the proton at position 7 in the tryptophan radical, etc.

Table 2 shows the dimensionless axially and biaxially parameters for each hyperfine tensor, defined as

Table 2

Axiality ( $\alpha$ ) and biaxiality ( $\beta$ ) parameters for nuclei in the flavin (FH $\cdot$ ) and tryptophan (W $\cdot$ ) radicals

Radical	Nucleus	$\alpha$	$\beta$
FH $\cdot$	N5	1.26	0.006
	N10	1.12	0.017
	H1'r	0.12	0.30
	H6	0.33	0.15
	H5	0.51	0.57
W $\cdot$	N1	0.83	0.00
	H5	0.44	0.31
	H7	0.42	0.33

$$\alpha = \frac{T_{33}}{2|a_{\text{iso}}|}, \quad \beta = \frac{T_{22} - T_{11}}{T_{33}}, \quad (7)$$

where  $T_{11}$ ,  $T_{22}$  and  $T_{33}$  represent the three principal components of the anisotropic part of the tensor (Table 1) and  $a_{\text{iso}}$  is the isotropic component of the tensor. Calculations were performed for three flavin–tryptophan radical pairs (**1**, **2** and **3**) with different selections of eight nuclear spins from the total of 10 (Table 3). The six nuclei with the largest isotropic hyperfine couplings and/or the largest anisotropy are included in all three radical pairs.

### 3. Background theory

Before presenting the results of the FH·W· simulations, we first summarize the predicted anisotropic magnetic field effects for a radical pair containing a single magnetic nucleus with spin quantum number  $I = 1/2$  [20]. For an axial hyperfine tensor, and a rate constant sufficiently small to allow extensive  $S \leftrightarrow T$  interconversion, a Low Field Effect is predicted. As the strength of the applied magnetic field is increased from zero, the singlet recombination probability  $\Phi_S$  falls sharply, reaches a minimum and then increases more gradually, rising above its zero field value. The position of the minimum in  $\Phi_S$  is determined principally by  $k$ : the longer lived the radical pair, the more abrupt the initial drop in  $\Phi_S$  and the lower the value of  $B_0$  at the minimum. In the presence of significant biaxiality, however, the LFE and the associated minimum are abolished, and  $\Phi_S$  rises as  $B_0$  is increased from zero. In addition, various resonances in  $\Phi_S$  are seen at  $B_0$ -values that lead to energy level crossings in the radical pair [20].

Table 3  
Nuclei included in calculations for the three radical pairs discussed in the text

Radical pair	FH·	W·
<b>1</b>	N5, N10, H1'r, H5	N1, H5, H7, H $\beta$ 2
<b>2</b>	N5, N10, H1'r, H6	N1, H5, H7, H $\beta$ 2
<b>3</b>	N5, N10, H1'r, H5, H6	N1, H5, H7

The anisotropic response to an applied magnetic field may be described more quantitatively in the limit of a very long lived one-proton radical pair subject to a magnetic field  $B_0$  that is either zero or very much weaker than all the energy level separations produced by the anisotropic hyperfine interaction. For an axial hyperfine tensor [20]:

$$\begin{aligned} \Phi_S^{\text{lim}}(B_0 = 0) &= \frac{3}{8}, \\ \Phi_S^{\text{lim}}(B_0 \neq 0) &= \frac{1}{4} + \frac{1}{8} \cos^2 \psi, \end{aligned} \quad (8)$$

where  $\psi$  is the angle between the direction of the magnetic field and the axis of the hyperfine interaction. The difference between  $\Phi_S^{\text{lim}}(B_0 = 0)$  and  $\Phi_S^{\text{lim}}(B_0 \neq 0)$  is the limiting depth of the low-field minimum in  $\Phi_S$ . The spherical average of  $\Phi_S^{\text{lim}}(B_0 \neq 0)$  is  $7/24$ , the limiting LFE is

$$I^{\text{lim}} = \frac{\Phi_S^{\text{lim}}(B_0 = 0) - \Phi_S^{\text{lim}}(B_0 \neq 0)}{\Phi_S^{\text{lim}}(B_0 = 0)} = \frac{1}{3} \sin^2 \psi \quad (9)$$

and the limiting anisotropy is

$$\begin{aligned} Q^{\text{lim}} &= \frac{\Phi_S^{\text{lim}}(B_0 \neq 0) - \langle \Phi_S^{\text{lim}}(B_0 \neq 0) \rangle}{\langle \Phi_S^{\text{lim}}(B_0 \neq 0) \rangle} \\ &= \frac{1}{7} (3 \cos^2 \psi - 1). \end{aligned} \quad (10)$$

The difference between the maximum and minimum values of  $\Phi_S^{\text{lim}}(B_0 \neq 0)$  divided by the spherical average is  $3/7$  or 43%. The results corresponding to Eqs. (8)–(10) for a radical pair initially in a triplet state are given in Appendix A.

The corresponding expressions are much simpler in the case of a biaxial tensor, for which there is no LFE

$$\Phi_S^{\text{lim}}(B_0 = 0) = \Phi_S^{\text{lim}}(B_0 \neq 0) = \frac{1}{4}. \quad (11)$$

The difference between the two cases stems from the nature of the electron–nuclear energy levels of the radical pair. The biaxial part of the hyperfine interaction removes the energy-level degeneracies produced by the axial component and so prevents a very weak applied magnetic field from inducing additional  $S \leftrightarrow T$  interconversion pathways [20]. Similar behaviour can be anticipated if the nucleus has spin quantum number  $I = 1$  instead of  $1/2$ . More complex orientation- and field-dependence

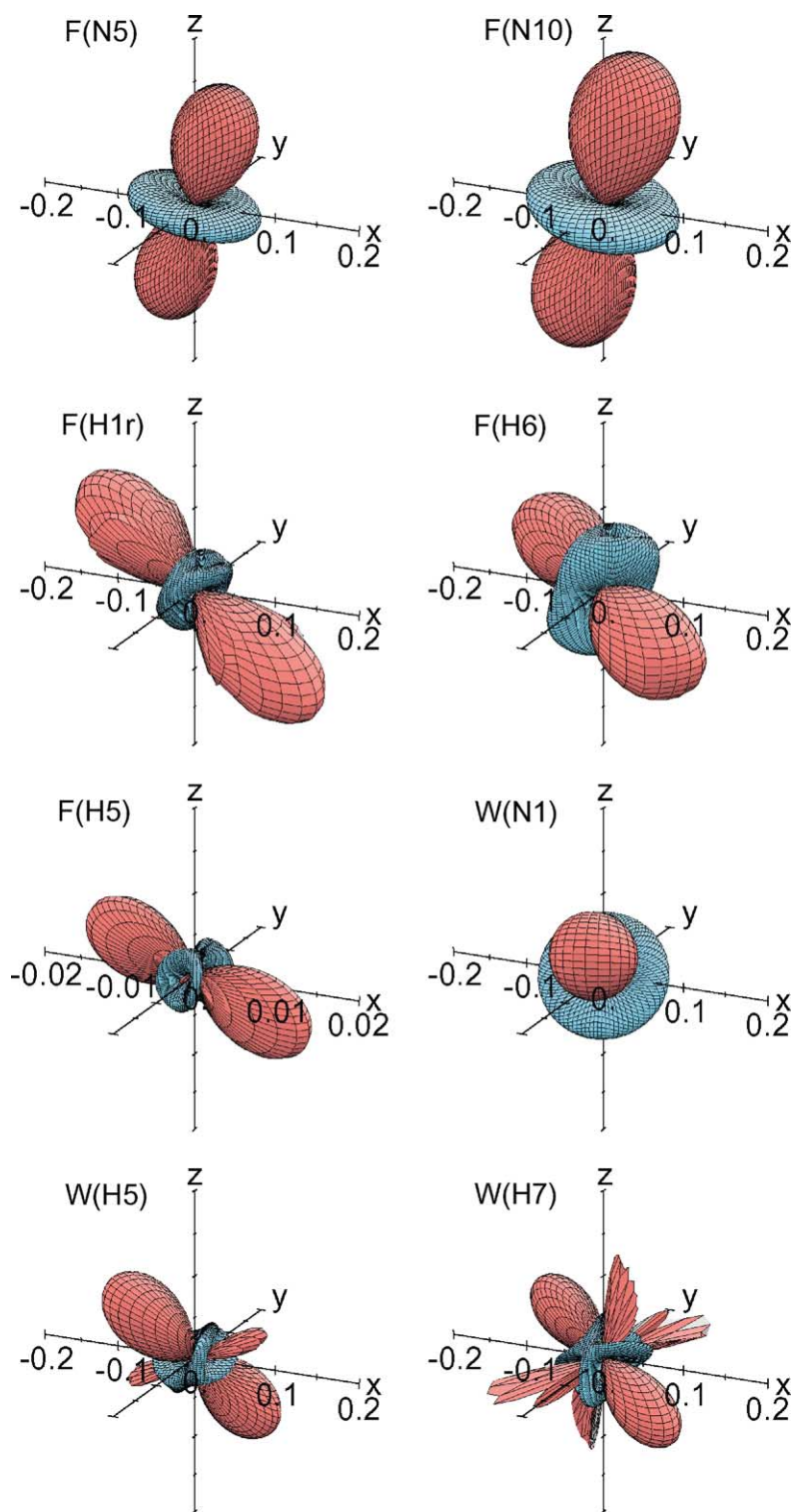


Fig. 3. The anisotropy of the calculated singlet recombination probability  $\Phi_S$  for eight radical pairs each containing a single magnetic nucleus, as indicated.  $B_0 = 50 \mu\text{T}$  and  $k = 2 \times 10^5 \text{ s}^{-1}$ .

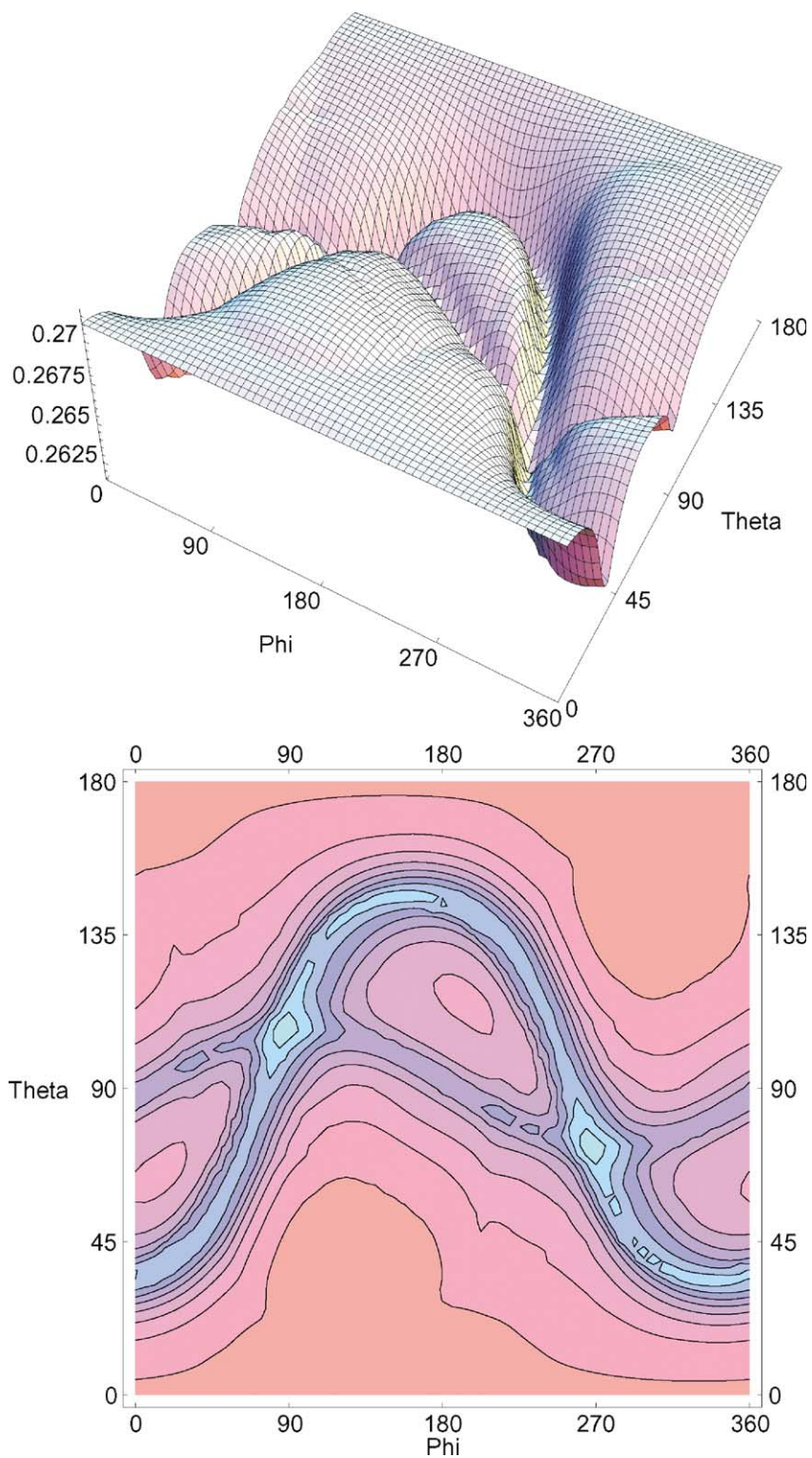


Fig. 4. Orientation dependence of the calculated singlet recombination probability  $\Phi_S$  for radical pair **1**.  $B_0 = 50 \mu\text{T}$  and  $k = 2 \times 10^5 \text{ s}^{-1}$ .

has been found for radical pairs containing two nuclear spins [24].

#### 4. Results

Fig. 3 shows the calculated  $\Phi_S$ -anisotropy for the eight individual nuclei in Table 1 that have anisotropic hyperfine interactions, i.e., for eight radical pairs each containing a single magnetic nucleus. The magnetic field is 50  $\mu\text{T}$  (approximately the strength of the geomagnetic field) and the lifetime of the radical pair is 5  $\mu\text{s}$  ( $k = 2 \times 10^5 \text{ s}^{-1}$ ). The coordinate system here and in Figs. 4–6 is as indicated in Fig. 2. With the exception of F(H5), which has the smallest  $\Phi_S$ -anisotropy (and the largest  $\beta$ , Table 2), the axes all span the range  $\{-0.2, 0.2\}$  in all three dimensions. Red and blue represent values of  $\Phi_S$  that are, respectively, larger than and smaller than the spherical average. The distance of the red or blue surface from the origin in any direction represents the deviation of  $\Phi_S$  from its spherical average, scaled by the spherical average, when  $B_0$  lies along that direction. There are three points to note. (a) The nuclei with hyperfine interactions that are closest to being axial (e.g., F(N5), F(N10) and W(N1)) show a  $\Phi_S$ -anisotropy approximating to  $3 \cos^2 \psi - 1$  where, as above,  $\psi$  is the angle between the direction of the applied magnetic field and the principal axis of the hyperfine tensor. This corresponds closely to the limiting behaviour in Eq. (10). Note that F(N5) and F(N10) have principal hyperfine axes in the flavin radical that are nearly collinear. (b) The deviations from  $3 \cos^2 \psi - 1$  orientation-dependence are most prominent for the nuclei with appreciable biaxiality (e.g., W(H5) and W(H7)). (c) The magnitude of the anisotropy for the axial and near-axial nuclei approaches that in Eq. (10), which predicts  $\Omega^{\text{lim}} = +2/7$  for  $B_0$  parallel to the hyperfine axis and  $-1/7$  for the perpendicular arrangement. The correspondence is not exact because neither  $k$  nor  $B_0$  are small enough for Eq. (10) to be strictly applicable (and because it applies only to spin-1/2 nuclei).

Extending the calculations to radical pair 1 (Table 3), with eight nuclear spins, one sees a more

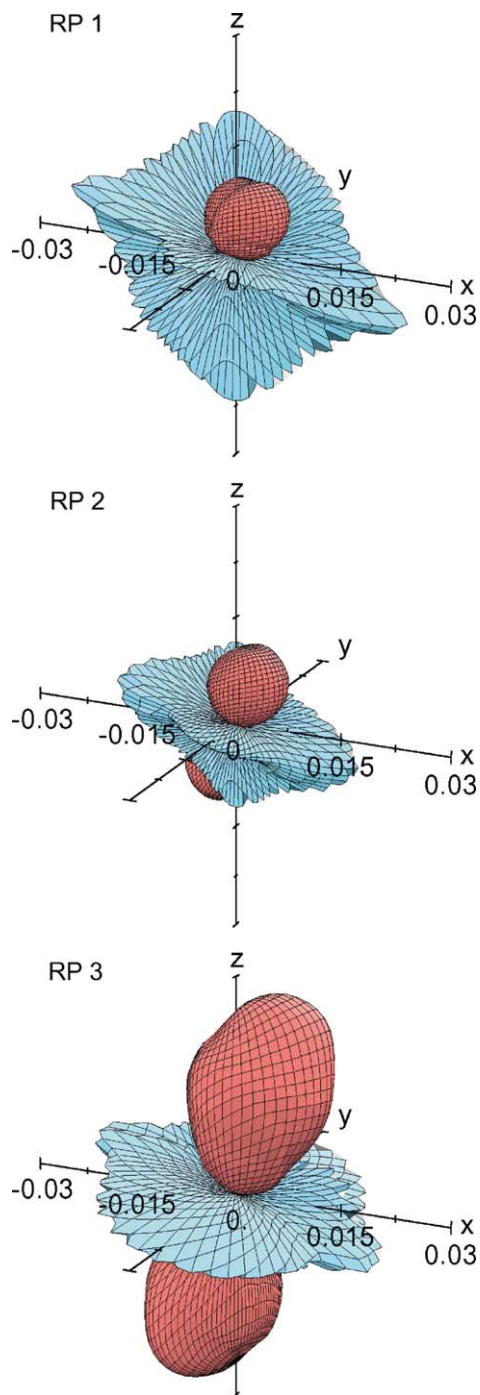


Fig. 5. The anisotropy of the calculated singlet recombination probability  $\Phi_S$  for radical pairs 1, 2 and 3.  $B_0 = 50 \mu\text{T}$  and  $k = 2 \times 10^5 \text{ s}^{-1}$ .

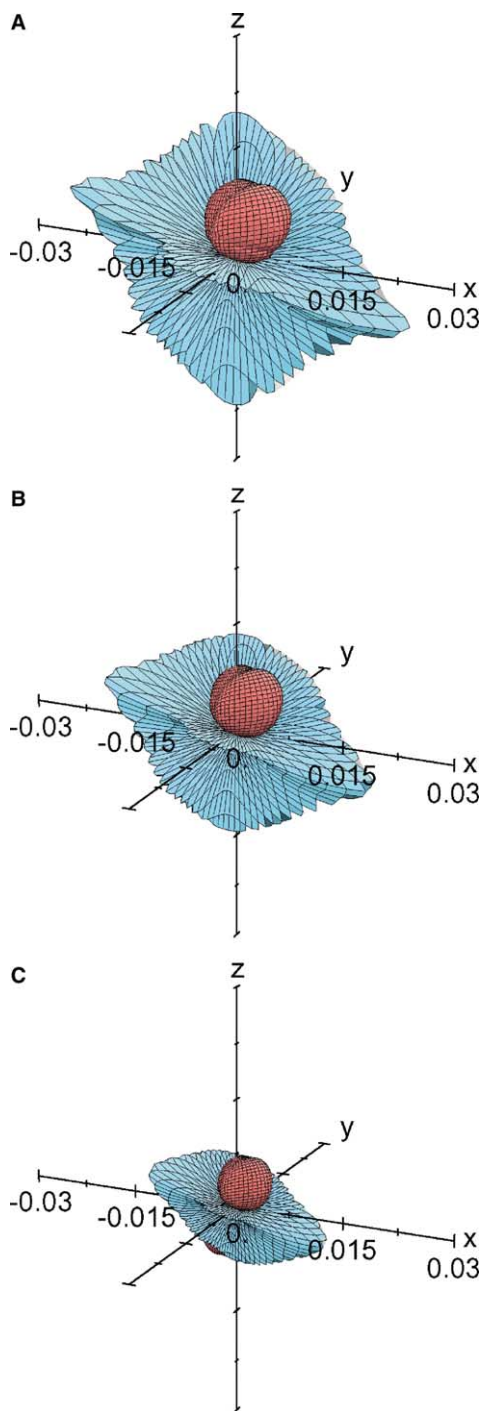


Fig. 6. The anisotropy of the calculated singlet recombination probability  $\Phi_S$  for radical pair **1** with (A)  $k = 2 \times 10^5 \text{ s}^{-1}$ , (B)  $k = 5 \times 10^5 \text{ s}^{-1}$  and (C)  $k = 1 \times 10^6 \text{ s}^{-1}$ .  $B_0 = 50 \text{ } \mu\text{T}$ .

complex anisotropy. Fig. 4 shows the orientation dependence of  $\Phi_S$  for  $B_0 = 50 \text{ } \mu\text{T}$  and  $k = 2 \times 10^5 \text{ s}^{-1}$ , both as a three-dimensional representation and as a contour plot. Although the variation in  $\Phi_S$  is not large – the maximum and minimum values are approximately 0.272 and 0.262 – the dependence on  $\theta$  and  $\phi$  is more intricate and far from monotonic. The surface representing  $\Phi_S$  is cut by two relatively deep sinuous intersecting valleys, most clearly seen in the contour plot. A measure of the anisotropy in  $\Phi_S$  is provided by the ratio of the difference between the maximum and minimum values of  $\Phi_S$  divided by the spherical average: in this case it is  $\sim 4\%$ . The anisotropic part of  $\Phi_S$  is shown in Fig. 5(A). The apparently large extent and jagged appearance of the negative (blue) feature derive from the ravine-like nature of the valleys (Fig. 4). Fig. 5 also shows the results of corresponding calculations for radical pairs **2** (B) and **3** (C). **1**, **2** and **3** differ in which two of the three nuclei F(H5), F(H6) and W(H $\beta$ 2) are included (Table 3). Although the exact choice of nuclei has a noticeable effect on  $\Phi_S$ , the general shape of the anisotropy is not greatly changed. Note that the axes in Fig. 5 all span the range  $\{-0.03, 0.03\}$  in all three dimensions. The anisotropies are 3.8%, 3.0% and 5.3% for A, B and C, respectively, i.e., less than an order of magnitude smaller than observed for the one-nucleus radical pairs in Fig. 3.

Fig. 6 shows the dependence of the recombination yield anisotropy on the recombination rate constant  $k$ , for radical pair **1**. As the lifetime of the radical pair is reduced from 5 to 2  $\mu\text{s}$  to 1  $\mu\text{s}$  ( $k = 2 \times 10^5, 5 \times 10^5, 1 \times 10^6 \text{ s}^{-1}$ ), the anisotropy of  $\Phi_S$  contracts by less than a factor of 2 and becomes smoother, without substantially changing in shape. This may also be seen in Fig. 7 where the field dependence of  $\Phi_S$  is shown for the same three rate constants. Here,  $\Phi_S$  is plotted for the two directions of the magnetic field that give maximum and minimum recombination yield in a 50- $\mu\text{T}$  magnetic field. As the lifetime is reduced,  $\Phi_S$  increases because there is less time for conversion of the initially formed singlet radical pair into the triplet state; the anisotropy shrinks for similar reasons. The “bumps” around 120 and 150  $\mu\text{T}$ ,

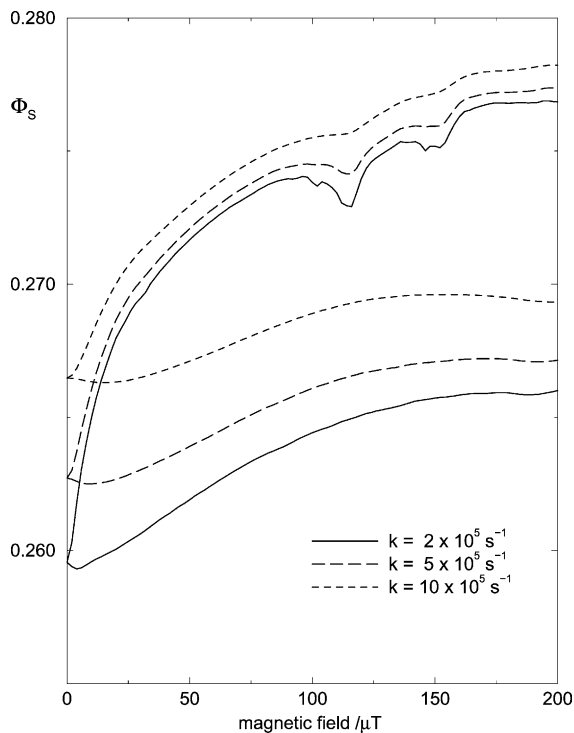


Fig. 7. Calculated singlet recombination probability for  $k = 2 \times 10^5 \text{ s}^{-1}$ ,  $5 \times 10^5 \text{ s}^{-1}$  and  $1 \times 10^6 \text{ s}^{-1}$  as a function of the strength of the applied magnetic field  $B_0$  for radical pair **1**. For each value of  $k$ , the values of  $\Phi_S$  are shown for the magnetic field directed along the lines of maximum and minimum  $\Phi_S$  at  $B_0 = 50 \text{ } \mu\text{T}$ .

which are most noticeable for the more slowly decaying radical pairs presumably arise from energy level-crossings [20].

## 5. Discussion

The product yields for the one-nucleus radical pairs depicted in Fig. 3 show a variety of anisotropies governed by the isotropic hyperfine coupling constant, the axially and biaxially of the hyperfine tensor and the directions of the tensor axes. In most cases, the extent of the anisotropy, judged as the difference between the maximum and minimum values of  $\Phi_S$  divided by the spherical average, is about half the theoretical maximum of 43%. This figure is reduced by less than an order of magnitude when the radical pair contains eight

nuclear spins instead of just one (Figs. 4 and 5). Given the variety of shapes displayed in Fig. 3 for the individual nuclei, it is perhaps surprising that the reduction in anisotropy is as small as this. Apparently, the anisotropies of the eight hyperfine tensors do not cancel one another as much as might have been expected.

It is clear from Fig. 5 that a radical pair compass is not sensitive to the polarity of the magnetic field, as previously noted by Ritz et al. [11]. If the direction of the field is reversed, the product yields are unchanged, i.e.  $\Phi_S(\theta, \phi) = \Phi_S(\theta + \pi, \phi)$ .

Fig. 5 also indicates that the magnitude of the anisotropy, but not its general shape, is sensitive to the exact combination of nuclear spins included in the calculation. The three radical pairs have six nuclei in common, with the addition of two of the three protons F(H5), F(H6) and W(H $\beta$ 2). The differences in anisotropic response for the three cases suggest that the magnetic properties of a radical pair compass could quite easily be tuned by variation of the tensors of a few of the nuclei, even those with relatively small hyperfine interactions.

The anisotropy in  $\Phi_S$  for radical pair **1** is not found to be strongly dependent on the rate of radical pair decay (Figs. 6 and 7). Reducing the lifetime from 5 to 2  $\mu\text{s}$  to 1  $\mu\text{s}$  changes the anisotropy from 3.7% to 3.0% to 2.2%. Smaller anisotropies can be expected for shorter lifetimes or if the electron spin correlation persists for less than a microsecond by virtue of rapid spin relaxation. At this point one might ask whether microsecond lifetimes are plausible for photoinduced radical pairs in proteins at room temperature. The evidence is limited, and lifetimes must clearly depend strongly on the nature of the radicals, the structure and dynamics of the protein and the proximity of any paramagnetic metal ions. However, long-lived radical pairs are known: the flavin–tryptophan radical pair in DNA photolyase, on which the present calculations are based, displays antiphase electron spin polarization for up to 20  $\mu\text{s}$  at 278 K, implying that both the radical pair and the correlation between the two electron spins persist for considerably longer than the 5  $\mu\text{s}$  used in the present calculations [42].

Fig. 7 also shows that there is no Low Field Effect for the FH·W· pair. The singlet recombina-

tion yield,  $\Phi_S$ , rises as  $B_0$  is increased from zero, rather than first decreasing as expected for anisotropic one-nucleus pairs and for multinuclear pairs in solution where the hyperfine anisotropy is averaged to zero by rapid rotational tumbling [16,20]. This is no doubt a consequence of the increased complexity of the spin Hamiltonian and the presence of significant biaxiality. Nevertheless,  $\Phi_S$  does show significant magnetic field dependence. For example, the variation of  $\Phi_S$  in the range  $50 \pm 25 \mu\text{T}$  is comparable to its dependence on  $\theta$  and  $\phi$ . This correspondence suggests that a flavin–tryptophan radical pair compass might only operate in a small range of magnetic field strengths around  $50 \mu\text{T}$  before it needs to be readjusted. Wiltshcko and Wiltshcko [52] have shown that the magnetic compass of European Robins that have been kept at  $46 \mu\text{T}$  is operative at  $43$  and  $54 \mu\text{T}$ , but that the birds are unable to orient at  $34$  and  $60 \mu\text{T}$  without adaptation. It is intriguing to note that a similar operative range is suggested by the  $\Phi_S$ -dependence of the flavin–tryptophan radical pair.

It is evident from the shape and orientation of the plots in Figs. 5 and 6 that the anisotropy in  $\Phi_S$  is dominated by the two nitrogens in the flavin, F(N5) and F(N10). These two are amongst the three nuclei (W(N1) is the other) that have, simultaneously, the largest axiality and the smallest biaxiality; F(N5) and F(N10) also happen to have hyperfine axes that are nearly collinear. Although it is, of course, difficult to generalise on the basis of a single instance, it is tempting to conclude that a condition for a significant anisotropic response from a multinuclear radical pair magnetoreceptor is that there should be a small number of strongly axial hyperfine interactions, with nearly collinear principal axes. Indeed, one may speculate that the  $\Phi_S$ -anisotropy of the radical pair studied here might be increased if the tryptophan radical were oriented relative to the flavin such that the hyperfine axis of W(N1), the third nucleus with large  $\alpha$  and small  $\beta$ , was aligned with those of F(N5) and F(N10). Thus, it may be that the cancellation effect referred to above for multinuclear systems can be offset by the reinforcement of the anisotropies of a few suitably oriented near-axial hyperfine tensors. These possibilities will be the focus of further work.

Further potential for evolutionary optimisation of a radical pair compass is provided by variations in the individual rate constants for recombination of singlet and triplet states, which are unlikely to be equal, and by the presence of weak spin–spin interactions between the radicals [16]. The involvement of electron–electron dipolar couplings in this context was proposed as long ago as 1986 by Arnold Hoff [53]. All these quantities are sensitive to the separation of the two radicals which could be used to tune the response of the magnetoreceptor to the geomagnetic field.

A further issue raised by Hoff is whether the anisotropic response of a radical pair-based compass would be of sufficient magnitude to make it a realistic proposition [53]. Clearly it is impossible to answer this question definitively, just as it was in 1986, without much more information than is currently available on the identity and location of the putative radical pair and on the signal transduction mechanism. However, one can ask whether a magnetic field-induced chemical change will stand out against stochastic fluctuations and so derive constraints for feasible models. Weaver et al. [54] recently applied such a signal-to-noise analysis to a general ligand–receptor model. They estimated that the number of neural receptors,  $R_T$ , required to overcome stochastic fluctuations is  $R_T \approx 4(\lambda_B \Delta B)^{-2}$ , where  $\lambda_B$  is a parameter characterizing the response of the sensory system to a small intensity change  $\Delta B$  around its operating point,

$$\lambda_B = \frac{1}{\Phi_S(B_0 = 50 \mu\text{T})} \left( \frac{d\Phi_S}{dB_0} \right)_{B_0=50 \mu\text{T}}. \quad (12)$$

Weaver et al. judged that a  $\lambda_B$  of  $100 \text{ T}^{-1}$  or larger is sufficient to design a chemically based sensor that can overcome stochastic noise. The FH·W· pair has  $\lambda_B$  approximately three times larger than this (for  $k = 2 \times 10^5 \text{ s}^{-1}$ ) and could thus work as a magnetic sensor for small changes in  $B_0$ . For a FH·W· sensor, the number of receptors required to detect a magnetic field anomaly of  $\Delta B = 10^{-7} \text{ T}$  is  $\sim 1 \times 10^9$ .

For a magnetic compass that detects small changes in orientation, the above expression for  $R_T$  needs to be modified by replacing  $\lambda_B \Delta B$  by  $\lambda_\theta \Delta \theta$  and  $B_0$  by  $\theta$  in Eq. (12) to obtain  $\lambda_\theta$ . Since  $\lambda_\theta$  is

$\sim 4 \times 10^{-4}$  degree $^{-1}$  for FH·W·, one finds that  $\sim 1 \times 10^7$  receptors would be required to detect a  $1^\circ$  change in orientation, and only  $\sim 1 \times 10^5$  for a  $10^\circ$  change. The FH·W· chemical magnetic sensor requires fewer receptors to detect small changes in orientation than to detect small magnetic field intensity changes and can be realized in a relatively small detector volume.

### Acknowledgements

This paper is dedicated to the memory of Arnold Hoff: we greatly miss his wisdom, insight and friendship. We are grateful to Friedhelm Lenzian for providing EPR and ENDOR data. P.J.H. thanks Brian Brocklehurst for helpful discussions and Ilya Kuprov for preparing Fig. 2. C.W.M.K. thanks Stefan Weber and Klaus Möbius for their support. This work has been supported by the Fetzer Institute, the Royal Society, the EMF Biological Research Trust, the EU (TMR Network Project FMRX-CT98-0214), the Volkswagen Foundation (Grant I/77100) and the Deutsche Forschungsgemeinschaft (Sonderforschungsbericht 498).

### Appendix A

The photoreaction in DNA photolyase on which the calculations presented in this paper are based proceeds via radical pairs formed in a *triplet* state. The limiting recombination yields for a one-proton pair in an initial triplet state may easily be derived from those presented in Section 3 for an initial *singlet* state and are given below:

$$\Phi_S^{\text{lim}}(B_0 = 0) = \frac{5}{24},$$

$$\Phi_S^{\text{lim}}(B_0 \neq 0) = \frac{1}{4} - \frac{1}{24} \cos^2 \psi,$$

$$\langle \Phi_S^{\text{lim}}(B_0 \neq 0) \rangle = \frac{17}{72},$$

$$\Gamma^{\text{lim}} = -\frac{1}{5} \sin^2 \psi,$$

$$\Omega^{\text{lim}} = -\frac{1}{17} (3 \cos^2 \psi - 1),$$

$$\frac{\max [\Phi_S^{\text{lim}}(B_0 \neq 0)] - \min [\Phi_S^{\text{lim}}(B_0 \neq 0)]}{\langle \Phi_S^{\text{lim}}(B_0 \neq 0) \rangle} = -\frac{3}{17}.$$

### References

- [1] A.J. Hoff, Q. Rev. Biophys. 14 (1981) 599.
- [2] U. Steiner, T. Ulrich, Chem. Rev. 89 (1989) 51.
- [3] M. Volk, A. Ogrodnik, M.E. Michel-Beyerle, in: R.E. Blankenship, M.T. Madigan, C.E. Bauer (Eds.), Anoxygenic Photosynthetic Bacteria, Kluwer, Dordrecht, 1995, p. 595.
- [4] J.R. Woodward, Prog. React. Kinet. Mec. 27 (2002) 165.
- [5] B. Brocklehurst, Chem. Soc. Rev. 31 (2002) 301.
- [6] D. Kuciauskas, P.A. Liddell, A.L. Moore, T.A. Moore, D. Gust, J. Amer. Chem. Soc. 120 (1998) 10880.
- [7] B. Brocklehurst, K.A. McLauchlan, Int. J. Radiat. Biol. 69 (1996) 3.
- [8] K. Schulten, C. Swenberg, A. Weller, Z. Phys. Chem. NF111 (1978) 1.
- [9] K. Schulten, in: J. Treusch (Ed.), Festkörperprobleme, vol. 22, Vieweg, Braunschweig, 1982, p. 61.
- [10] K. Schulten, A. Windemuth, in: G. Maret, J. Kiepenheuer, N. Boccara (Eds.), Biophysical Effects of Steady Magnetic Fields, Springer, Berlin, 1986, p. 99.
- [11] T. Ritz, S. Adem, K. Schulten, Biophys. J. 78 (2000) 707.
- [12] D.T. Edmonds, Proc. R. Soc. B 263 (1996) 295.
- [13] J.L. Kirschvink, M.M. Walker, C.E. Diebel, Curr. Opin. Neurobiol. 11 (2001) 462.
- [14] T. Ritz, D.H. Dommer, J.D. Phillips, Neuron 34 (2002) 503.
- [15] R. Wiltchko, W. Wiltchko, Animal Behav. 65 (2003) 257.
- [16] C.R. Timmel, U. Till, B. Brocklehurst, K.A. McLauchlan, P.J. Hore, Molec. Phys. 95 (1998) 71.
- [17] B. Brocklehurst, J. Chem. Soc. Faraday Trans. II 72 (1976) 1869.
- [18] S.N. Batchelor, C.W.M. Kay, K.A. McLauchlan, I.A. Shkrob, J. Phys. Chem. 97 (1993) 13250.
- [19] U. Till, C.R. Timmel, B. Brocklehurst, P.J. Hore, Chem. Phys. Lett. 298 (1998) 7.
- [20] C.R. Timmel, F. Cintolesi, B. Brocklehurst, P.J. Hore, Chem. Phys. Lett. 334 (2001) 387.
- [21] G. Feher, R.A. Isaacson, M.Y. Okamura, W. Lubitz, in: M.E. Michel-Beyerle (Ed.), Antennas and Reaction Centers of Photosynthetic Bacteria, Springer, Berlin, 1985, p. 174.
- [22] F. Lenzian, W. Lubitz, H. Scheer, C. Bubenzer, K. Möbius, J. Am. Chem. Soc. 103 (1981) 4635.
- [23] Y. Miyamoto, A. Sancar, Proc. Natl. Acad. Sci. USA 95 (1998) 6097.

- [24] F. Cintolesi, C.R. Timmel, unpublished work.
- [25] B. Brocklehurst: personal communication.
- [26] S.-T. Kim, A. Sancar, *Photochem. Photobiol.* 57 (1993) 895.
- [27] A. Sancar, *Biochemistry* 33 (1994) 2.
- [28] A. Sancar, *Science* 272 (1996) 48.
- [29] P.F. Heelis, R.F. Hartman, S.D. Rose, *Chem. Soc. Rev.* 24 (1995) 289.
- [30] P.F. Heelis, R.F. Hartman, S.D. Rose, *J. Photochem. Photobiol. A Chem.* 95 (1996) 89.
- [31] X. Zhao, D. Mu, *Histol. Histopathol.* 13 (1998) 1179.
- [32] T. Todo, *Mutat. Res.* 434 (1999) 89.
- [33] J. Deisenhofer, *Mutat. Res.* 460 (2000) 143.
- [34] C.L. Thompson, A. Sancar, *Oncogene* 21 (2002) 9043.
- [35] G.B. Sancar, *Mutat. Res.* 451 (2000) 25.
- [36] H.-W. Park, S.-T. Kim, A. Sancar, J. Deisenhofer, *Science* 268 (1995) 1866.
- [37] P.F. Heelis, A. Sancar, *Biochemistry* 25 (1986) 8163.
- [38] Y.M. Gindt, E. Vollenbroek, K. Westphal, H. Sackett, A. Sancar, G.T. Babcock, *Biochemistry* 38 (1999) 3857.
- [39] M.S. Cheung, I. Daizadeh, A.A. Stuchebrukhov, P.F. Heelis, *Biophys. J.* 76 (1999) 1241.
- [40] C. Aubert, P. Mathis, A.P.M. Eker, K. Brettel, *Proc. Natl. Acad. Sci. USA* 96 (1999) 5423.
- [41] C. Aubert, M.H. Vos, P. Mathis, A.P.M. Eker, K. Brettel, *Nature* 405 (2000) 586.
- [42] C.W.M. Kay, H. Mögling, E. Schleicher, K. Hitomi, K. Möbius, T. Todo, A. Bacher, G. Richter, S. Weber, in: S. Chapman, R. Perham, N. Scrutton (Eds.), *Flavins and Flavoproteins*, Rudolf Weber Agency for Scientific Publications, Berlin, 2002, p. 713.
- [43] P.J. Hore, D.A. Hunter, C.D. McKie, A.J. Hoff, *Chem. Phys. Lett.* 137 (1987) 495.
- [44] S. Weber, C.W.M. Kay, H. Mögling, K. Möbius, K. Hitomi, T. Todo, *Proc. Natl. Acad. Sci. USA* 99 (2002) 1319.
- [45] R. Brudler, K. Hitomi, H. Daiyasu, H. Toh, K. Kucho, M. Ishiura, M. Kanehisa, V.A. Roberts, T. Todo, J.A. Tainer, E.D. Getzoff, *Molec. Cell* 11 (2003) 59.
- [46] T. Tamada, K. Kitadokoro, Y. Higuchi, K. Inaka, A. Yasui, P.E. de Ruiter, A.P.M. Eker, K. Miki, *Nature Struct. Biol.* 4 (1997) 887.
- [47] H. Komori, R. Masui, S. Kuramitsu, S. Yokoyama, T. Shibata, Y. Inoue, K. Miki, *Proc. Natl. Acad. Sci. USA* 98 (2001) 13560.
- [48] C.W.M. Kay, R. Feicht, K. Schulz, P. Sadewater, A. Sancar, A. Bacher, K. Möbius, G. Richter, S. Weber, *Biochemistry* 38 (1999) 16740.
- [49] S. Weber, K. Möbius, G. Richter, C.W.M. Kay, *J. Am. Chem. Soc.* 123 (2001) 3790.
- [50] M.J. Frisch et al., *Gaussian 98 (Revision A.7)*, Gaussian, Inc., Pittsburgh, PA, 1998.
- [51] F. Lendzian, M. Sahlin, F. MacMillan, R. Bittl, R. Fiege, S. Pötsch, B.-M. Sjöberg, A. Gräslund, W. Lubitz, G. Lassmann, *J. Amer. Chem. Soc.* 118 (1996) 8111.
- [52] W. Wiltchko, R. Wiltchko, *Science* 176 (1972) 62.
- [53] A.J. Hoff, E.J. Lous, in: G. Maret, J. Kiepenheuer, N. Boccara (Eds.), *Biophysical Effects of Steady Magnetic Fields*, Springer, Berlin, 1986, p. 74.
- [54] J.C. Weaver, T.E. Vaughan, R.D. Astumian, *Nature* 405 (2000) 707.